IEEE Access
Multidisciplinary | Rapid Review | Open Access Journal

Received 20 May 2024, accepted 26 June 2024, date of publication 2 July 2024, date of current version 10 July 2024.

Digital Object Identifier 10.1109/ACCESS.2024.3422255

RESEARCH ARTICLE

Adaptive Estimation Using Interacting Multiple Model With Moving Window

AHSAN SAEEDZADEH[1], PEYMAN SETOODEH[1], (Senior Member, IEEE), MARJAN ALAVI[2], (Senior Member, IEEE), AND SAEID HABIBI[1], (Member, IEEE)

[1]Department of Mechanical Engineering, McMaster University, Hamilton, ON L8S 4L8, Canada
[2]W. Booth School of Engineering Practice and Technology, Hamilton, ON L8S 4L8, Canada

Corresponding author: Ahsan Saeedzadeh (Saeedzaa@mcmaster.ca)

This work was supported by the Natural Sciences and Engineering Research Council of Canada (NSERC) under Grant RGPIN-2020-05735.

ABSTRACT State estimation is paramount in control, monitoring, and fault management across various domains. Uncertainty in model parameters and changing system dynamics pose significant challenges to accurate state estimation. This paper proposes a novel adaptive estimation strategy called the Moving Window Interacting Multiple Model (MWIMM). Using a moving window improves identifiability and computational efficiency of the multiple model algorithms by focusing on a subset of possible models, rather than considering all models at each stage. MWIMM enables the estimation of gradual changes in the system, making it valuable for fault intensity and Remaining Useful Life (RUL) estimation. The paper provides an overview of adaptive estimation strategies, presents the formulation of MWIMM for fault intensity and RUL estimation, and investigates the parameter estimation problem. Results are compared with those of augmented state Extended Kalman Filter (EKF) estimation, and it is shown that the proposed MWIMM approach offers a promising alternative for effectively handling extensive parameter uncertainty and accommodating gradual changes in system parameters.

INDEX TERMS Adaptive estimation, moving window IMM, fault diagnosis, RUL estimation.

I. INTRODUCTION

State estimation is an essential step in various fields, including control, monitoring, fault management [1], [2] and control of cyber-physical systems [3]. However, system states may be partially observable or even unobservable. In addition to the challenges posed by the unknown states, another important barrier in state estimation is the uncertainty within the model parameters. Since these parameters are often not precisely known, the estimation process is inherently unpredictable and imprecise. Moreover, system dynamics gradually change over time due to aging. It is also possible that a system undergoes abrupt changes, which include switching in the entire system dynamics. Hybrid models are deployed to capture this phenomenon. In such cases, estimating the model parameters alongside the states becomes particularly valuable, as it aids in detecting faults and predicting their future behavior as well as allowing for proactive maintenance and management.

State estimation accuracy heavily depends on the prior knowledge of model parameters. When parameters are precisely known, which is unrealistic in most applications, the Kalman Filter (KF) offers optimal state estimation for linear systems assuming zero-mean Gaussian noise [1]. Furthermore, in the presence of small parametric uncertainties, the impact of parameter mismatch is typically insignificant compared to the process noise, enabling the KF to maintain a satisfactory performance [4]. However, for scenarios involving moderate parametric uncertainty, alternative approaches become necessary. One approach involves introducing artificial white noise by increasing specific elements of the process noise covariance matrix, Q,

The associate editor coordinating the review of this manuscript and approving it for publication was Jiajie Fan.

within the KF algorithm [4]. Another technique adaptively adjusts the process noise covariance matrix by monitoring residuals within the KF [5]. Alternatively, a robust estimation strategy such as the Smooth Variable Structure Filter (SVSF) with Variable Boundary Layer (SVSF-VBL) optimizes estimation error while considering parametric uncertainty through deploying a switching gain [6], [7].

In the presence of significant parametric uncertainty, the traditional approach of increasing process noise and treating it as equivalent to white noise within the KF becomes inadequate. In this case, the effects of parametric uncertainties become significant and cannot be considered as added white noise [4]. Although SVSF can guarantee boundedness of estimation error in the presence of large uncertainties, it requires a large corrective gain, which leads to chattering [8], [9]. While the mean error may decrease rapidly due to this significant gain, the excessive control action can result in a large Root Mean Square Error (RMSE) for SVSF [10]. As an alternative, particle filters are known nonlinear filtering techniques suitable for more general systems characterized by unknown uncertainties and non-Gaussian probability density functions (PDFs). However, their performance is contingent on the number of particles employed and they require very high computational power. An infinite number of particles would be necessary for the estimation error to converge to zero in an ideal setting [11].

Joint state and parameter estimation offers an alternative approach for dealing with extensive parametric uncertainties and for accommodating gradual changes in model parameters. However, this method presents challenges due to its reliance on nonlinear filtering and calls for solving complex nonlinear Partial Differential Equations (PDEs) to obtain the optimal solution. The augmented state Extended Kalman Filter (EKF) provides a suboptimal solution [12], which is susceptible to bias estimation and divergence for several reasons [13], [14]. Firstly, the augmented states lack meaningful dynamics, making it challenging to intuitively select the artificially introduced noise based on engineering guesses [4]. Secondly, discriminative training methods for determining the process noise covariance matrix depend on measured states, and including augmented states can negatively impact the training process [5], [15]. Additionally, validity of linearization used in the EKF becomes compromised in the presence of significant parametric uncertainty. Moreover, incorporating augmented states can render the system unobservable [12].

Alternatively, adaptive estimation strategies offer a different viewpoint that tackles significant uncertainties and enables the estimation of abrupt changes in the system that are a possible occurrence in hybrid systems and fault detection scenarios. In this paper, a novel adaptive estimation strategy is developed based on the Interacting Multiple Model (IMM) method. The new algorithm called Moving Window Interacting Multiple Model (MWIMM) offers the following advantages compared to the traditional IMM algorithm:

- It is capable of estimating gradual changes in system parameters, making it valuable for fault prognosis and Remaining Useful Life (RUL) estimation problems. This is achieved through utilizing parameter bins.
- It improves computational efficiency and avoids combinatorial explosion, which are two common problems associated with MMAE algorithms including traditional IMM strategy. This is accomplished by narrowing down the search space to a specific window rather than considering all potential models at each stage.
- It relaxes the assumed irreversible condition used in the Updated IMM (UIMM) algorithm [16], [17], [18], thus extending its application to a wider range of problem domains.

The paper follows the subsequent structure: Section II presents an overview of adaptive estimation strategies. In Section III, the formulation of MWIMM for fault intensity and remaining useful life estimation is presented. Section IV investigates the application of the proposed MWIMM in a comprehensive parameter estimation problem, comparing the results with parameter estimation using augmented state extended Kalman filter. Section V explores the influence of three crucial factors—identifiability, optimality, and system excitation—on the performance of the multiple model adaptive estimation strategy in general and the proposed method specifically. It is demonstrated through a case study that for a Multiple Model Adaptive Estimation (MMAE) strategy, observability of all models in the filter bank does not guarantee identifiability. Finally, the paper concludes with summarizing remarks in the last section.

II. BACKGROUND: ADAPTIVE ESTIMATION STRATEGY

Adaptive estimation using multiple models for hypothesis testing, known as Multiple Model Adaptive Estimation (MMAE), proves to be a valuable tool for handling large parameter uncertainty and hybrid systems characterized by different system models with distinct parameter sets [4]. MMAE assumes that engineering knowledge can serve as prior information about the hybrid models and the feasible range of parameters. This approach enables the estimation of system states while providing an algorithm to identify changing parameters or the true underlying model. MMAE finds extensive applications in real-time problems, including autonomous vehicles [19], [20], target tracking [21], [22], fault diagnosis [23], [24], [25], and fault-tolerant control systems [16], [26], [27], [28]. The multiple model estimation procedure involves three main steps: generating individual state estimates that correspond to a given parameter vector, evolving the hypothesis probability, and combining the individual estimates.

In the realm of MMAE, two distinct approaches can be observed: static and dynamic. Static MMAE assumes the exclusive usage of a single model throughout the entire process, without any transitions or jumps occurring. Consequently, it is unsuitable for time-variant systems characterized by changing parameters or instances where the

system switches between different models. On the other hand, dynamic MMAE is specifically designed for time-varying systems and proves to be well-suited for online fault diagnosis or target tracing applications [1]. Notably, within the realm of dynamic MMAE, three widely recognized strategies are the General Pseudo-Bayesian estimator of the first order (GPB1), the General Pseudo-Bayesian estimator of the second order (GPB2), and the Interacting Multiple Model (IMM). Among these, IMM gained interest due to its reported computational efficiency while maintaining a performance comparable to that of GPB2 [1]. As a result, IMM emerges as a promising choice for dynamic MMAE applications. Hence, the proposed method in this study is built on IMM.

III. MOVING WINDOW INTERACTIVE MULTIPLE MODEL FOR FAULT INTENSITY AND REMAINING USEFUL LIFE ESTIMATION

The novel Moving Window Interactive Multiple Model (MWIMM) strategy is proposed and is well-suited for addressing problems characterized by a gradual progression of degradation, such as estimating a system's Remaining Useful Life (RUL) and measuring fault intensity. Assessment of RUL involves evaluating the level of degradation in a system and estimating its remaining operational lifespan, with the estimation of battery State of Health (SoH) being a prominent example. Precise fault intensity measurement is a fundamental pillar in prognostics and condition monitoring applications. Taking account of the inherent chronological order involved in these issues, the MWIMM strategy can effectively estimate RUL and quantify fault intensity, incorporating supplementary temporal information to enhance computational efficiency, and improve identifiability compared to the IMM strategy. Consider a general linear system that is subject to switching as described below:

$$\begin{aligned}\mathbf{x}(k) &= \mathbf{A}(M(k))\mathbf{x}(k-1) + \mathbf{B}(M(k))\mathbf{u}(k) \\ &\quad + \mathbf{v}(k-1, M(k)), \qquad (1)\\ \mathbf{z}(k) &= \mathbf{C}\left(M\left(k\right)\right)\mathbf{x}(k) + \mathbf{D}\left(M\left(k\right)\right)\mathbf{u}(k) \\ &\quad + \mathbf{w}\left(k, M\left(k\right)\right). \qquad (2)\end{aligned}$$

In this context, $\mathbf{x}(k)$ and $\mathbf{z}(k)$ are state and measurement vectors respectively, $M(k)$ represents the true model at time k, while $\mathbf{A}\left(M\left(k\right)\right)$, $\mathbf{B}\left(M\left(k\right)\right)$, $\mathbf{C}\left(M\left(k\right)\right)$, and $\mathbf{D}\left(M\left(k\right)\right)$ refer to the system matrices associated with model $M(k)$. Additionally, $\mathbf{v}\left(k-1, M\left(k\right)\right)$ and $\mathbf{w}\left(k, M\left(k\right)\right)$ represent the process and measurement noise corresponding to model $M(k)$, respectively. These systems are also known as jump-linear systems, assuming that the mode jump process exhibits left continuity [1]. This means that the influence of the new model initiates from time k onwards. The vector $\mathbf{x}(k)$, which takes on continuous values, and the discrete variable $M(k)$ are sometimes denoted as the base state and modal state, respectively [1].

The model at time k is assumed to be among the N possible fault severity levels as:

$$M\left(k\right) \in \left\{M_{FL[i]}\right\}_{i=0}^{N-1}, \qquad (3)$$

where the subscript $FL[i]$ stands for the fault intensity level of "i". A larger "i" means the model has a more severe fault (i.e., the model $M_{FL[0]}$ corresponds to a healthy system or zero fault intensity level, and model $M_{FL[i]}$ has the fault intensity level of "i"). Similarly for RUL estimation, $M(k)$ is assumed to be among the N possible RUL levels as:

$$M(k) \in \left\{M_{RUL[i]}\right\}_{i=0}^{N-1}. \qquad (4)$$

Here, the index "i" serves as an indicator of the system's level of degradation. For instance, the model $M_{RUL[0]}$ corresponds to zero degradation or the maximum RUL, while the model $M_{RUL[i]}$ represents the RUL level associated with the degradation level "i" of the system. In a general formulation applicable to all level-based model sets, such as fault intensity level sets or RUL level sets, (3) and (4) can be expressed as follows:

$$M(k) \in \left\{M_{L[i]}\right\}_{i=0}^{N-1}. \qquad (5)$$

In this context,$M_{L[i]}$ represents the model corresponding to level "i". Assuming that the model switching follows a Markov process with a known mode transition, a common assumption in MMAE strategies leads to the following [1]:

$$p_{ij} := P\left\{M\left(k\right) = M_{L[j]} \middle| M(k-1) = M_{L[i]}\right\}. \qquad (6)$$

The mode transition probabilities, represented by p_{ij}, are constant over time and independent of the base state. To account for the inherent temporal information associated with the chronological order, it is possible to build the transition matrix assuming that the transition probability increases when the model levels are in close proximity, as illustrated in (7):

$$|i-j_1| < |i-j_2| \;\rightarrow\; p_{ij_1} > p_{ij_2}. \qquad (7)$$

In contrast to the IMM strategy, the MWIMM approach utilizes a filter bank that includes only neighboring models of the matched model, incorporating information aligned with the chronological order. Consequently, the number of filters operating in parallel depends on the chosen size of the moving window that defines the neighborhood. As illustrated in Fig. 1, when a model transition occurs, signifying a change in the matched model, the moving window adjusts accordingly. Regarding the initial condition, it is reasonable to assume that the system is in a healthy state (level zero) at the commencement of the process. However, the proposed algorithm can start from any other initial condition.

Remark 1: In cases where the true model is not included within the model bank contained in the window employed by the MWIMM approach, an automatic adjustment takes place. Such cases can occur due to incorrect initial conditions or a significant and abrupt change during the process that pushes the model outside the window. The adjustment process involves initial convergence towards the "nearest" model [29], followed by the subsequent sliding of the window's position.

Remark 2: In general, it is advisable to opt for an odd-sized window in the MWIMM framework, with the

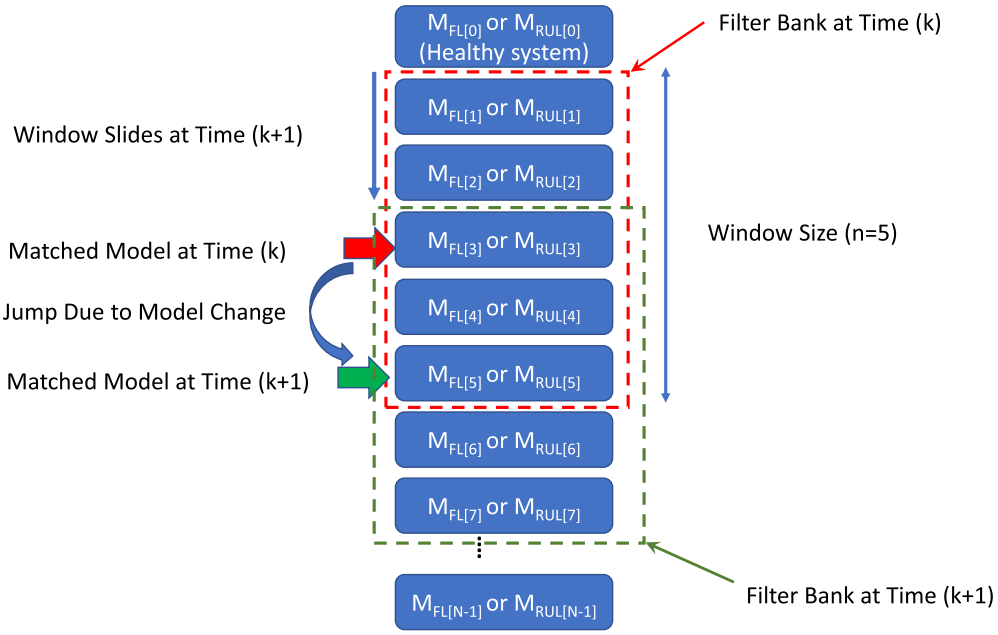

FIGURE 1. Flowchart illustrating the MWIMM approach for estimating RUL and addressing fault intensity issues.

matched model positioned at the center. This choice helps prevent any bias towards switching to higher or lower levels. However, depending on the application, it is permissible to employ a skewed window that tilts toward a specific direction. For instance, in the case of RUL estimation, where switching consistently occurs in the direction of lower RUL due to the nature of aging, the MWIMM design can incorporate a skewed window that promotes switching predominantly in that specific direction.

Remark 3: The applicability of the MWIMM strategy extends to nonlinear systems by employing linearization techniques, following the same underlying principles utilized in the IMM strategy [1].

Remark 4: The computational efficiency of the MWIMM approach is enhanced by reducing the number of running filters, number of combinations and number of probability calculations in comparison to the IMM strategy. This improvement is demonstrated in Table. 1, where "n" represents the size of the moving window and "N" denotes the total number of models. The same strategy can be applied to GPB1 and GPB2 estimators using targeted moving windows, known as MWGPB1 and MWGPB2 respectively, in Table. 1, resulting in improved computational efficiency.

Based on Remark 1, it can be inferred that selecting a window of size $n = 3$ with the matched model in the center is generally adequate since the MWIMM strategy adjusts the window position over time to encompass the true model. However, in situations where the model levels are closely spaced, resulting from selecting small bin levels, and the system undergoes rapid changes, the sliding window may lag behind and fail to converge to include the true model in a timely manner. Increasing the window size addresses this issue by sacrificing computational efficiency (as shown in Table. 1), but it facilitates the inclusion of the true model within the sliding window and expedites convergence. Further elaboration on these issues will be provided in the subsequent section, which discusses the selection of MWIMM parameters for parameter estimation problems.

IV. MOVING WINDOW INTERACTIVE MULTIPLE MODEL FOR PARAMETER IDENTIFICATION

The MWIMM strategy can be applied in a general context for parameter identification tasks when system parameters are unknown and potentially subject to time variations. Consider a general linear system as follows, with parameter $\theta(k)$ being unknown and time-varying:

$$\begin{aligned}\mathbf{x}(k) &= \mathbf{A}\left(\theta\left(k\right)\right)\mathbf{x}(k-1) + \mathbf{B}\left(\theta\left(k\right)\right)\mathbf{u}(k) \\ &\quad + \mathbf{Q}\left(\theta\left(k\right)\right)\mathbf{v}(k-1), \qquad (8)\\ \mathbf{z}(k) &= \mathbf{C}\left(\theta\left(k\right)\right)\mathbf{x}(k) + \mathbf{D}\left(\theta\left(k\right)\right)\mathbf{u}(k) \\ &\quad + \mathbf{R}\left(\theta\left(k\right)\right)\mathbf{w}(k), \qquad (9)\end{aligned}$$

where $\mathbf{A}\left(\theta\left(k\right)\right)$, $\mathbf{B}\left(\theta\left(k\right)\right)$, $\mathbf{C}\left(\theta\left(k\right)\right)$, and $\mathbf{D}\left(\theta\left(k\right)\right)$ represent system matrices, $\mathbf{Q}\left(\theta\left(k\right)\right)$ and $\mathbf{R}\left(\theta\left(k\right)\right)$ denote the matrices associated with process noise and measurement noise, respectively, as functions of $\theta(k)$. Without loss of generality $\theta(k)$ is assumed to be bounded as follows:

$$\beta_1 \leq \theta(k) \leq \beta_2, \qquad (10)$$

Then, the set of models can be created based on discretizing the value of $\theta\left(k\right)$ to N bins as:

$$\begin{aligned}\theta_i &:= \beta_1 + \frac{2i+1}{2N}\left(\beta_2 - \beta_1\right)\\ &\text{where } i \in \{0, 1, \ldots, N-1\}, \qquad (11)\\ M(k) &\in \left\{M_{L[\theta_i]}\right\}_{i=0}^{N-1}, \qquad (12)\end{aligned}$$

TABLE 1. A comparative analysis of computational requirements among various MMAE strategies.

Adaptive Estimation Strategy	#Combinations	#Filters	#Probability Calculations
IMM [1]	$N+1$	N	N^2+N
MWIMM	$n+1$	n	n^2+n
GPB1 [1]	1	N	N
MWGPB1	1	n	n
GPB2 [1]	$N+1$	N^2	N^2+N
MWGPB2	$n+1$	n^2	n^2+n

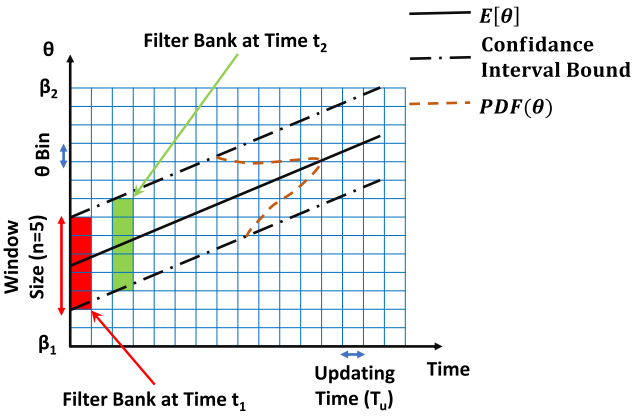

FIGURE 2. Parameter identification using the MWIMM strategy.

where θ_i represents the central value of the ith bin, and $M_{L[\theta_i]}$ corresponds to the model associated with parameter θ_i, which can be derived based on (8) and (9). The total number of models (N) depends on the chosen bin size for θ_i. Thus, identification of parameter θ entails determining the model $M(k)$ in (12), which can be solved using the MWIMM strategy. Opting for a smaller bin size enhances the resolution for identification of θ; however, this leads to closely spaced $M_{L[\theta_i]}$ models, posing a greater challenge for MWIMM in terms of identification. Fig. 2 illustrates the application of MWIMM in a parameter identification context for estimating a time-varying parameter. This figure highlights the importance of two additional parameters: the window size and the updating time for the MWIMM sliding window. Remark 1 suggests that a window size of $n = 3$, with the matched model positioned in the center, is generally sufficient. However, for improved performance, the window size can be determined by considering the confidence interval of the Probability Density Function (PDF), if such information is available (as depicted in Fig. 2). The impact of the updating time and bin size will be extensively investigated in the following section through several case studies.

Remark 5: If the probability distribution function of the parameter to be identified (θ) is available, the transition matrix for the MWIMM strategy can be formed accordingly.

Remark 6: The aforementioned approach can also be applied for identification of multiple parameters by utilizing a parameter vector ($\boldsymbol{\theta}$), whereby the number of models grows exponentially with respect to the number of parameters to be identified.

A. CASE STUDY: SECOND ORDER SYSTEM PARAMETER IDENTIFICATION

This section utilizes the MWIMM strategy with the Kalman Filter as the underlying filter (referred to as MWIMM-KF) to estimate the natural frequency of a second-order system. Assuming that only the first state has been measured, the state-space model (13) represents a generic second-order system with parameters such as damping ratio ζ, natural frequency ω_0, measurement noise $\mathbf{w}(k)$, and process noise $\mathbf{v}(k)$:

$$\begin{cases} x_1(k+1) = x_1(k) + T_s x_2(k) + v_1(k) \\ x_2(k+1) = -T_s\omega_0^2 x_1(k) + (1 - 2T_s\zeta\omega_0)\, x_2(k) \\ \qquad\quad +T_s b u(k) + v_2(k), \end{cases}$$
$$z(k) = x_1(k) + w(k), \tag{13}$$

where T_s denotes the time-step and u is the system input. Let us assume that the parameters of the system are specified as follows: $\zeta = 0.1, b = 100$, uncorrelated process noise $v_1(k) \sim \mathcal{N}\left(0,\ 10^{-12}\right)$ and $v_2(k) \sim \mathcal{N}\left(0, 10^{-6}\right)$, and measurement noise $w(k) \sim \mathcal{N}\left(0, 10^{-10}\right)$. Given that the system behavior changes gradually over time due to variations in the natural frequency, the MWIMM strategy can be employed to estimate the natural frequency. In this approach, a window size of three is chosen, limiting the consideration to three models in the filter bank at each instant. To ensure a high resolution, the bin size for the natural frequency is set to 0.05 Hz. The sampling time used in the filter is $0.002s$, while the updating time bin for the sliding window (T_u) is 1s. The transition matrix $\mathbf{P}_{ij}$, initial mode probability $\boldsymbol{\mu}(0)$, and mode probability threshold for sliding $\mu_{Threshold}$, are determined as follows:

$$\mathbf{P}_{ij} = \begin{bmatrix} 0.9 & 0.05 & 0.05 \\ 0.05 & 0.9 & 0.05 \\ 0.05 & 0.05 & 0.9 \end{bmatrix}, \quad \boldsymbol{\mu}(0) = \begin{bmatrix} 0.25 \\ 0.5 \\ 0.25 \end{bmatrix},$$
$$\mu_{Threshold} = 0.5. \tag{14}$$

The threshold for the mode probability in the sliding window reflects the sliding window's sensitivity to model transitions. A higher threshold value makes the MWIMM window reluctant to slide, thereby minimizing false transitions caused by noise. However, it also reduces the sensitivity of the estimation to parameter changes. In this case study, a threshold of 0.5 is chosen to ensure that sliding occurs only when the new "matched model" has the highest probability among the model banks. The minimum threshold can be set as

the maximum mode probability at each time step to establish a reference level.

The covariance matrices used for the Kalman filter are derived from the measurement and process noises in the following manner:

$$\mathbf{Q} = \begin{bmatrix} 10^{-12} & 0 \\ 0 & 10^{-6} \end{bmatrix}, \quad \mathbf{R} = 10^{-10}, \\ \mathbf{P}(0|0) = \begin{bmatrix} 1 & 0 \\ 0 & 1 \end{bmatrix}. \tag{15}$$

The results illustrated in Fig. 3 show the MWIMM-KF's effective estimation of both states, while successfully identifying the gradual change in the natural frequency. With a chosen window size of three ($n = 3$), Fig. 3a displays three mode probabilities: "Model Low," "Model Mid," and "Model Up," corresponding to models with lower, middle, and higher natural frequencies within the window. When the mode probability of "Model Up" surpasses the others (t between 25s and 125s), it signifies an increasing natural frequency, prompting an upward slide of the MWIMM window. Conversely, when the mode probability of "Model Low" exceeds the others (from $t = 175s$ to $t = 275s$), it indicates a decreasing natural frequency, causing the window to slide downward. Finally, when the mode probability of "Model Mid" outweighs the others ($t \leq 25s$ or $125s \leq t \leq 175s$ or $275s \leq t$), it signifies a constant natural frequency, resulting in the window to remain stationary. In Fig. 3b, the estimated natural frequency exhibits step levels with a resolution of 0.05 Hz, derived from the chosen frequency bin in the MWIMM models.

To achieve the same level of resolution (0.05 Hz) with traditional IMM, assuming the upper and lower bound of natural frequency are known to be 2 and 4 Hz respectively, 40 filters needed to be run simultaneously, compared to the 3 filters used in the MWIMM approach. Based on Table. 1, the number of probability calculations needed for the IMM algorithm becomes 1640 compared to 10 calculations needed for the MWIMM. Therefore, it is computationally infeasible to estimate the natural frequency with the same resolution using the traditional IMM. Even with access to substantial computational power, accuracy would be an issue due to the combinatorial effect of the 1640 hypotheses that must be handled in each step. One approach to make the IMM feasible is to decrease the resolution. For example, given similar computational resources, the IMM resolution would be 1 Hz (20 times less accurate than MWIMM used here), while it still needs an extra assumption that the upper and lower bounds are known. Consequently, the IMM algorithm in its current format is inadequate for estimating gradual parameter changes. An alternative method involves employing joint state and parameter estimation techniques, such as the augmented state Kalman filter. This approach results in a system of partial differential equations that are difficult to solve and may make the system unobservable. Further elaboration on this issue can be found in Section V.

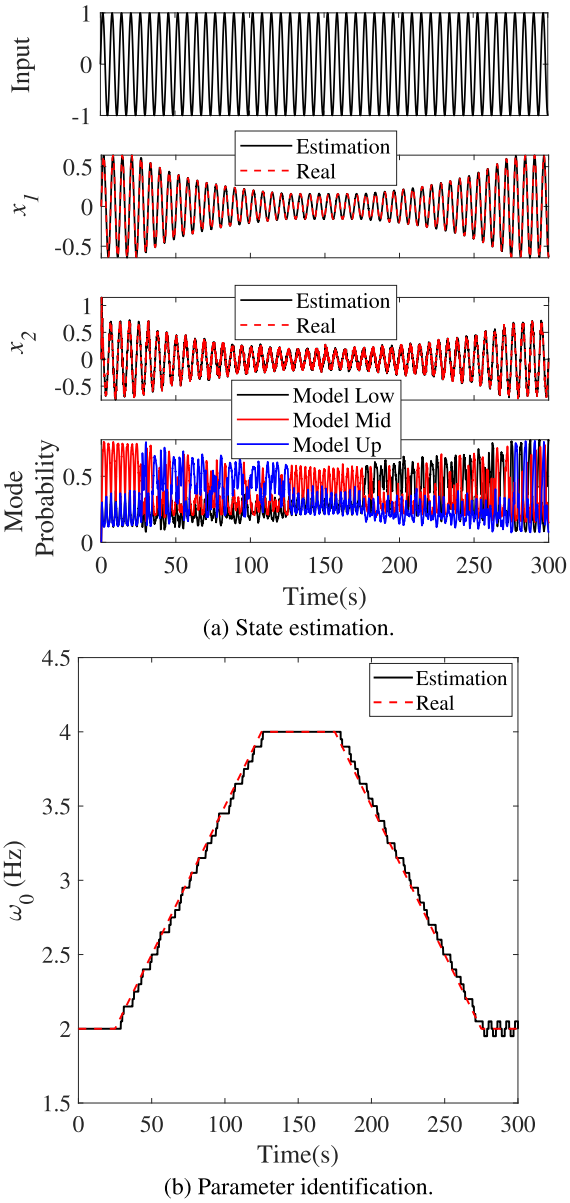

(a) State estimation.

(b) Parameter identification.

FIGURE 3. Using MWIMM-KF for estimating the time-varying parameter of a second-order system.

1) EFFECT OF BIN SIZE AND UPDATING TIME

The choice of bin size within the MWIMM strategy significantly impacts the process of parameter estimation by influencing both the accuracy and convergence of the estimation. A smaller bin size enhances the resolution of the estimated parameter, allowing for finer details to be captured. However, when a parameter undergoes rapid changes, MWIMM with a small bin size will slide the window of the filter bank slower than the rate of parameter change and will fail to converge to the true value in a timely manner. This issue is shown in Figure 4, where Bin1 demonstrates a scenario in which the MWIMM strategy lacks sufficient time to effectively track the gradual change in the target parameter. To address this challenge, one potential solution is to increase the window size ($n > 3$), allowing for a

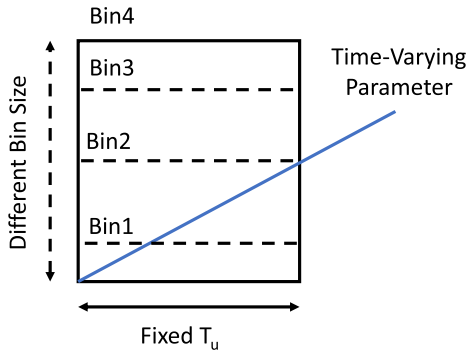

FIGURE 4. Schematic depiction of the effect of the rate of change of a parameter on determining an appropriate bin size.

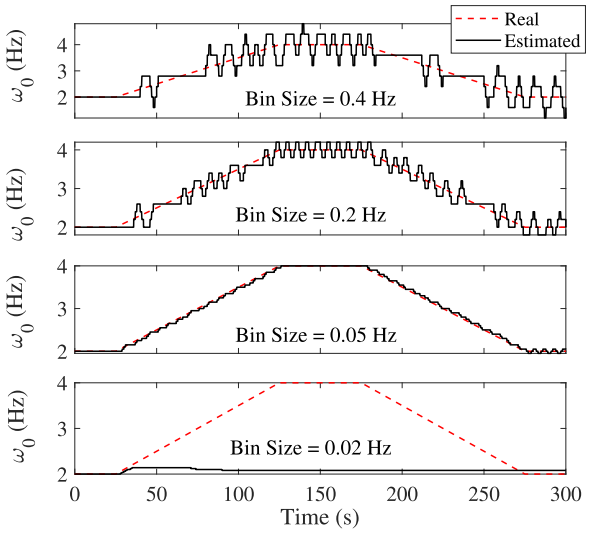

FIGURE 5. Estimating natural frequency for different bin sizes.

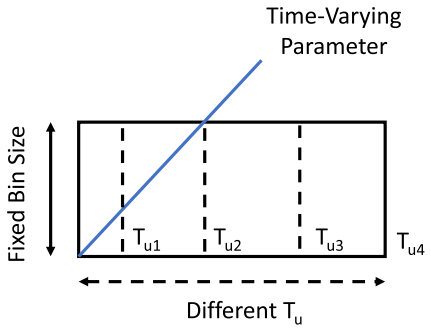

FIGURE 6. Schematic depiction of the effect of the rate of change of a parameter on determining an appropriate updating time.

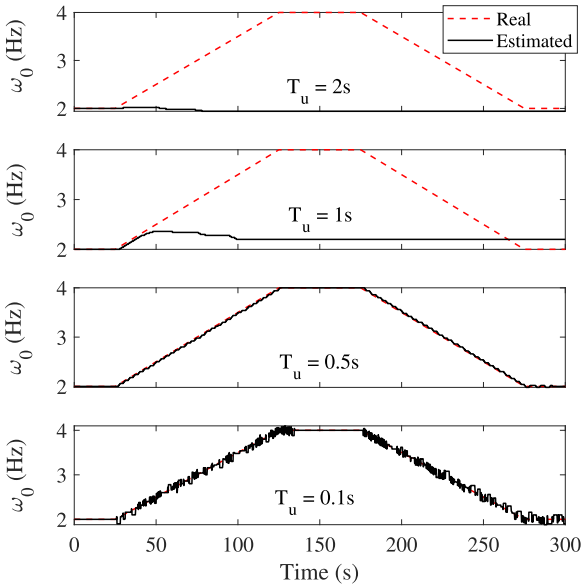

FIGURE 7. Estimating natural frequency for different updating times.

larger interval to be covered in each update. Nevertheless, this approach necessitates running more filters in parallel, leading to increased computational demand and a higher risk of combinatorial explosion [16]. Additionally, employing a small bin size diminishes the difference between the models in the filter bank, and potentially further escalates the risk of combinatorial explosion.

In Figure 5, the natural frequency estimation of the previously introduced second-order system is performed using different bin sizes under the exact same conditions. It is evident that larger bin sizes, such as 0.4 Hz and 0.2 Hz, lead to a deterioration in the resolution of the parameter estimation. On the other hand, employing a very small bin size of 0.02 Hz causes the MWIMM strategy to lag behind and ultimately fail in accurately estimating the natural frequency.

These observations highlight the trade-off involved in selecting an appropriate bin size in MWIMM. A balance must be struck between achieving higher resolution and ensuring timely convergence to the true parameter value. The choice of bin size should be tailored to the specific characteristics of the parameter being estimated and the dynamics of the system under investigation.

Employing a longer updating time in the MWIMM increases the amount of measurement data available for estimating the correct model, thereby reducing the likelihood of false switching, and yielding smoother parameter estimation results. However, when the rate of change of the parameter is high, MWIMM with a longer updating time, as demonstrated in Fig. 6 for updating T_{u3} and T_{u4}, tends to lag behind. In Fig. 7, estimation of the natural frequency is conducted for the previously introduced second-order system using various updating times while maintaining a fixed bin size of 0.02 Hz. As depicted in this figure, a smaller updating time of 0.1s results in higher fluctuations in the estimated natural frequency, as expected. Conversely, larger updating times such as 1s and 2s cause the MWIMM to be unable to keep pace with the rapid rate of change in the natural frequency.

B. IDENTIFYING BOTH NATURAL FREQUENCY AND DAMPING RATIO

One alternative approach for estimating the natural frequency involves utilizing joint state and parameter estimation. This

technique considers the natural frequency as an augmented state within the system and employs a nonlinear filter, such as the Extended Kalman Filter (EKF), to estimate it alongside other states, as long as the system maintains observability. However, it is important to note that this method provides a suboptimal solution, and the accuracy of the linearization is compromised when there is significant uncertainty in the parameters. By considering the natural frequency as an augmented state in the system described in (13), it is possible to prove observability of the system using Lie derivative. Consequently, the natural frequency can be estimated using the EKF estimation method. In this section, the EKF-based MWIMM method (MWIMM-EKF) is applied to identify the damping ratio and the natural frequency of a second-order system, thereby demonstrating the applicability of the MWIMM approach for nonlinear systems as well.

Regarding the natural frequency as an augmented state, we can reformulate the model in (13) as follows:

$$\begin{cases} x_1(k+1) = x_1(k) + T_s x_2(k) + v_1(k) \\ x_2(k+1) = -T_s x_3^2(k) x_1(k) + (1 - 2T_s \zeta x_3(k))\, x_2(k) \\ \qquad\quad + T_s b u(k) + v_2(k) \\ x_3(k+1) = x_3(k) + v_3(k), \end{cases}$$
$$z(k) = x_1(k) + w(k), \tag{16}$$

State variable x_3, which represents the natural frequency, incorporates artificial noise $v_3(k) \sim \mathcal{N}(0, 10^{-6})$. The MWIMM employs the same parameters as described in (14). However, here, the set of considered models is formed according to the discretization of the damping ratio, and model validation is performed using the estimated value of the damping ratio at each time step. To ensure accurate resolution, a bin size of 0.05 is chosen for the damping ratio. Moreover, when considering the augmented state vector, covariance matrices of the EKF are updated as follows:

$$\mathbf{Q} = \begin{bmatrix} 10^{-12} & 0 & 0 \\ 0 & 10^{-6} & 0 \\ 0 & 0 & 10^{-6} \end{bmatrix}, \quad \mathbf{R} = 10^{-10},$$
$$\mathbf{P}(0|0) = \begin{bmatrix} 1 & 0 & 0 \\ 0 & 1 & 0 \\ 0 & 0 & 1 \end{bmatrix}. \tag{17}$$

From (16), the measurement function can be obtained as $h(x) = x_1$. The observability matrix can then be computed utilizing Lie derivatives in the following manner:

$$\mathcal{O}(x,u) = \begin{bmatrix} dL_f^0 h(x) \\ dL_f^1 h(x) \\ \cdots \\ dL_f^{n-1} h(x) \end{bmatrix} = \begin{bmatrix} 1 & 0 & 0 \\ 0 & 1 & 0 \\ x_3^2 & 2\zeta x_3 & 2\zeta x_2 + 2x_3 x_1 \end{bmatrix}. \tag{18}$$

Here, $dL_f^n h$ represents the nth order Lie derivative of the measurement function h with respect to the system model f,

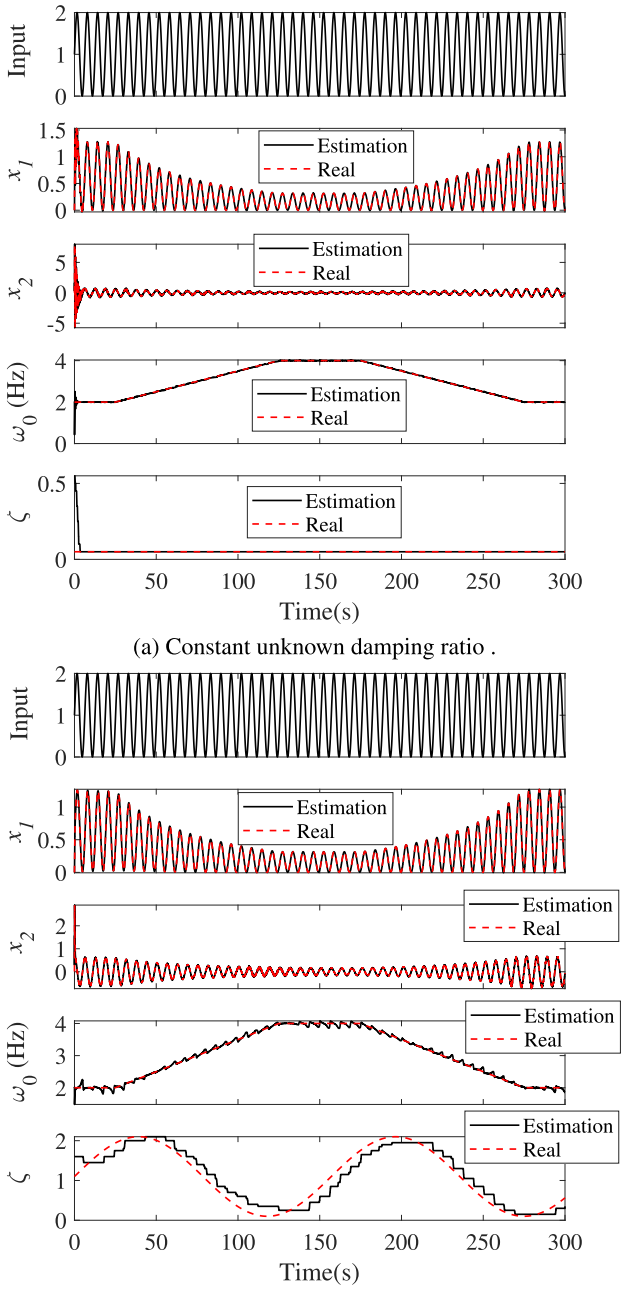

(a) Constant unknown damping ratio .

(b) Time-varying damping ratio.

FIGURE 8. Estimating natural frequency and damping ratio using MWIMM-EKF.

and $\mathcal{O}$ represents the observability matrix. The observability matrix is full rank as long as $2\xi x_2 + 2x_3 x_1$ is not equal to zero. It means that the system is observable. The only scenario for the system to be unobservable is when both states x_1 and x_2 are zero (trivial solution for any linear system) which is very rare and can be ignored. Fig. 8 demonstrates that the MWIMM-EKF accurately estimates natural frequency, damping ratio, and system states, including scenarios with both constant and unknown damping ratios (Fig. 8a) as well as time-varying damping ratios (Fig. 8b).

For comparative analysis, in this section, the augmented state EKF is employed to estimate both natural frequency and

damping ratio along with other states. Therefore, equation 13 can be reformulated as follows:

$$\begin{cases} x_1(k+1) = & x_1(k) + T_s x_2(k) + v_1(k) \\ x_2(k+1) = & -T_s x_3^2(k) x_1(k) + (1 - 2T_s x_4(k)\, x_3(k)) \\ & x_2(k) + T_s b u(k) + v_2(k) \\ x_3(k+1) = & x_3(k) + v_3(k) \\ x_4(k+1) = & x_4(k) + v_4(k), \end{cases}$$
$$z(k) = x_1(k) + w(k), \tag{19}$$

where x_3 is natural frequency and x_4 is damping ratio. In order to ensure a fair comparison, all conditions in this section are assumed to be identical to those in the previous section. However, there is one distinction regarding the artificial noise v_4 corresponding to damping ratio x_4. Obtaining this artificial noise for the augmented state EKF is not straightforward due to the lack of information about the dynamics of the augmented states. Consequently, it becomes challenging to intuitively select the noise based on engineering guesswork [4], and employing discriminative training methods is ineffective for determining the process noise for all four states using only one measurement x_1.

Assuming that the damping ratio can fluctuate with a standard deviation of 0.01, an added artificial noise is assumed with the normal distribution of $v_4(k) \sim \mathcal{N}\left(0, 10^{-4}\right)$. Covariance matrices of the EKF are then derived as follows:

$$\mathbf{Q} = \begin{bmatrix} 10^{-12} & 0 & 0 & 0 \\ 0 & 10^{-6} & 0 & 0 \\ 0 & 0 & 10^{-6} & 0 \\ 0 & 0 & 0 & 10^{-4} \end{bmatrix}, \quad \mathbf{R} = 10^{-10},$$
$$\mathbf{P}(0|0) = \begin{bmatrix} 1 & 0 & 0 & 0 \\ 0 & 1 & 0 & 0 \\ 0 & 0 & 1 & 0 \\ 0 & 0 & 0 & 1 \end{bmatrix}. \tag{20}$$

The observability matrix can then be computed using Lie derivatives as (21), shown at the bottom of the next page.

As shown, it is not necessarily guaranteed that the observability matrix is full rank, indicating that in general, observability cannot be proven and the system is only partially observable. Fig. 9 illustrates that the augmented state EKF fails to estimate both constant and time-varying damping ratios.

V. DISCUSSION AND FUTURE DIRECTIONS

To comprehensively investigate the performance of the Multiple-Model Adaptive Estimation (MMAE) strategy, particularly the Moving Window IMM (MWIMM) proposed in this paper, it is essential to carefully examine three key factors. These factors play a crucial role in understanding the efficacy of these strategies:

1) Identifiability: This factor evaluates the ability of the MMAE strategy to accurately identify the true model among the bank of possible models. It is important to note that even if all the models within the bank are observable, identifiability cannot be guaranteed. The absence of identifiability indicates the singularity of the Fisher information matrix, and vice versa [30]. In such cases, it becomes necessary to incorporate a priori information by imposing constraints on the model or consider reparameterization of the model as a potential solution.
2) Optimality: Theoretically speaking, optimality can be guaranteed only in the case of static MMAE, where the system has time-invariant parameters [4]. For dynamic multiple-model adaptive estimation strategies such as Interacting Multiple Models (IMM) and MWIMM, which deal with systems with time-varying parameters, only suboptimal solutions can be obtained.
3) System Excitation: To accurately estimate time-varying parameters, the system under study needs to be excited. This excitation is necessary for convergence towards the true model. Therefore, to maintain observability, careful consideration should be given to the level of system excitation, especially for nonlinear systems.

Understanding these factors can significantly contribute to the development and evaluation of effective estimation strategies in various applications. In the following section, an illustrative example is presented to show the identifiability challenge encountered in dynamic multiple-model adaptive estimation.

Consider a second-order system, exemplified by a mass-spring-damper configuration, which is derived by an external force F as:

$$\begin{cases} x_1(k+1) = x_1(k) + T_s x_2(k) + v_1(k) \\ x_2(k+1) = -T_s \omega_0^2 x_1(k) + (1 - 2T_s \zeta \omega_0)\, x_2(k) \\ \qquad +T_s b u(k) + v_2(k) - T_s F, \end{cases}$$
$$z(k) = x_2(k) + w(k). \tag{22}$$

Using the previously mentioned parameter values, including a natural frequency of $2Hz$, a damping ratio of 0.1, a value of b equivalent to 100, uncorrelated process noise $v_1(k) \sim \mathcal{N}\left(0,\ 10^{-12}\right)$, and $v_2(k) \sim \mathcal{N}\left(0, 10^{-6}\right)$. Now considering the availability of velocity measurement for the second state, subject to measurement noise $w(k) \sim \mathcal{N}\left(0, 10^{-8}\right)$. Additionally, assume the external force F to possess three distinct levels, namely low ($50N$), mid ($500N$), and high ($2000N$). System observability is assessed as follows:

$$\mathbf{C} = \begin{bmatrix} 0 & 1 \end{bmatrix}, \quad \mathbf{A} = \begin{bmatrix} 0 & 1 \\ -\omega_0^2 & -2\zeta\omega_0 \end{bmatrix} \tag{23}$$
$$\Longrightarrow \mathcal{O} = \begin{bmatrix} \mathbf{C} \\ \mathbf{CA} \end{bmatrix} = \begin{bmatrix} 0 & 1 \\ -\omega_0^2 & -2\zeta\omega_0 \end{bmatrix} \Longrightarrow \textit{full rank}. \tag{24}$$

The observability matrix with full rank indicates that the system is observable, allowing for unique determination of states x_1 and x_2. Nevertheless, as demonstrated in the

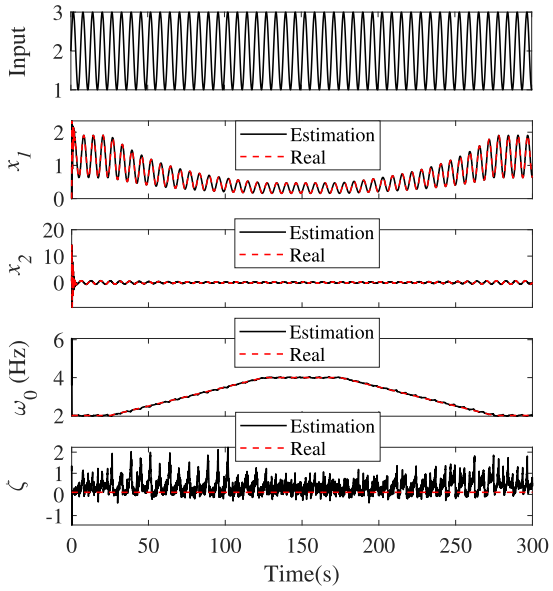

(a) Constant unknown damping ratio .

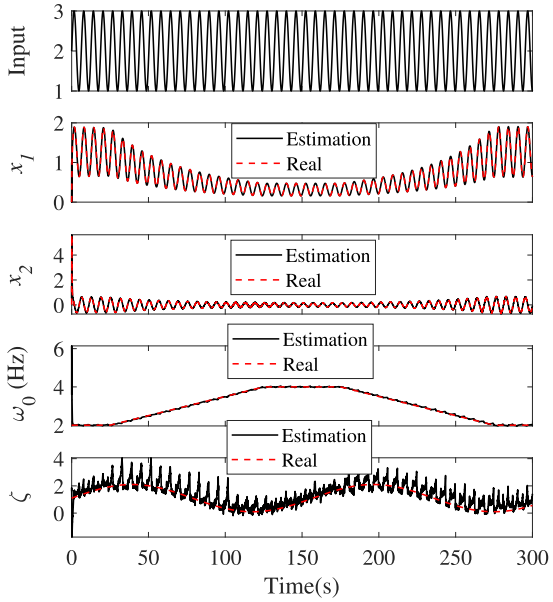

(b) Time-varying damping ratio.

FIGURE 9. **Estimating natural frequency and damping ratio using Augmented state EKF.**

following illustration, the external force cannot be estimated as an augmented state using the KF due to the system's lack of observability.

$$\begin{cases} x_1(k+1) = x_1(k) + T_s x_2(k) + v_1(k) \\ x_2(k+1) = -T_s\omega_0^2 x_1(k) + (1 - 2T_s\zeta\omega_0)\, x_2(k) \\ \qquad -T_s x_3(k) + T_s b u(k) + v_2(k) \\ x_3(k+1) = x_3(k) + v_3(k), \end{cases}$$
$$z(k) = x_2(k) + w(k). \tag{25}$$

In (25), the augmented state x_3 represents the external force. To perform the observability test, the observability matrix can be derived as follows:

$$\boldsymbol{C} = \begin{bmatrix} 0 & 1 & 0 \end{bmatrix}, \quad \boldsymbol{A} = \begin{bmatrix} 0 & 1 & 0 \\ -\omega_0^2 & -2\zeta\omega_0 & -1 \\ 0 & 0 & 0 \end{bmatrix}$$
$$\Rightarrow \boldsymbol{\mathcal{O}} = \begin{bmatrix} \boldsymbol{C} \\ \boldsymbol{CA} \\ \boldsymbol{CA}^2 \end{bmatrix} = \begin{bmatrix} 0 & 1 & 0 \\ -\omega_0^2 & -2\zeta\omega_0 & -1 \\ 2\zeta\omega_0^3 & \left(4\zeta^2 - 1\right)\omega_0^2 & 2\zeta\omega_0 \end{bmatrix} \tag{26}$$
$$\Rightarrow Rank\,(\boldsymbol{\mathcal{O}}) = 2 \quad \Rightarrow \boldsymbol{\mathcal{O}}\ is\ not\ full\ rank.$$

According to (26), it is evident that the system lacks observability, thereby preventing the estimation of the external force using the augmented KF. To address this issue, an alternative approach is IMM-KF. This method involves incorporating models for low, mid, and high external forces, and leveraging the mode probability to determine the true model at each time step, thereby enabling the identification of the external force. To assess the effectiveness of this approach, a series of events is considered as a simulation scenario:

1) For the initial 10 seconds, the external force is set to a low level ($F = 50N$).
2) From 10 seconds to 20 seconds, the external force transitions to a mid-level ($F = 500N$).
3) Finally, for the last 10 seconds, the external force switches to a high level ($F = 2000N$).

Fig. 10 demonstrates that the IMM-KF fails to accurately estimate the state x_1 and cannot correctly identify the external force, despite each model in the filter bank being individually observable based on (24). However, as depicted in Fig. 11 and Fig. 12, the IMM-KF can successfully estimate the states and identify the external force accurately when either the measurement for state x_1 or both states are available. Overall, Fig. 12 illustrates that the IMM-KF achieves the

$$\mathcal{O}(x,u) = \begin{bmatrix} dL_f^0 h(x) \\ dL_f^1 h(x) \\ \cdots \\ dL_f^{n-1} h(x) \end{bmatrix}$$
$$= \begin{bmatrix} 1 & 0 & 0 & 0 \\ 0 & 1 & 0 & 0 \\ x_3^2 & 2x_4x_3 & 2x_3x_1 + 2x_2x_4 & 2x_2x_3 \\ 2x_3^3x_4 & 4x_3^2x_4^2 + x_3^2 & 8x_3x_4^2x_2 + 6x_3^2x_4x_1 + 2x_2x_3 + 2bx_4u & 8x_4x_3^2x_2 + 2x_3^3x_1 + 2bx_3u \end{bmatrix}. \tag{21}$$

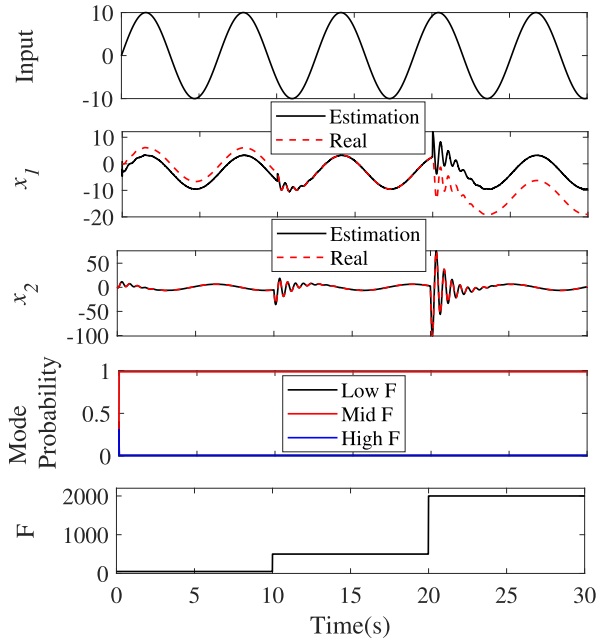

FIGURE 10. Identifying the external force for a second-order system with measurement feedback from x_2 using IMM-KF.

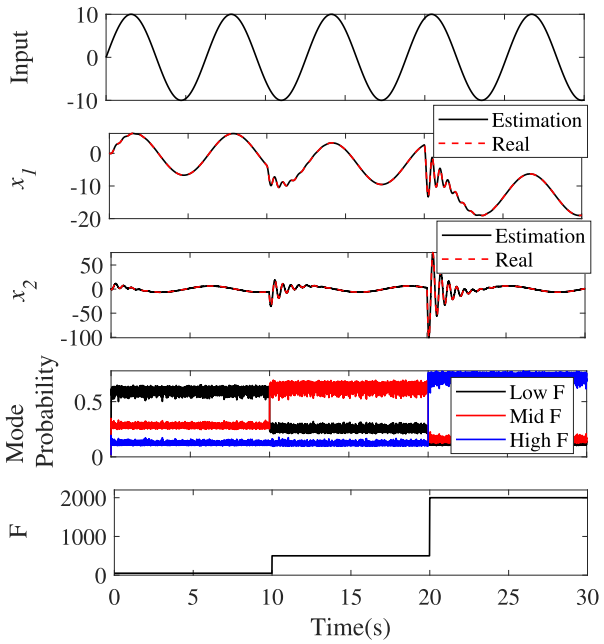

FIGURE 11. Identifying the external force for a second-order system with measurement feedback from x_1 using IMM-KF.

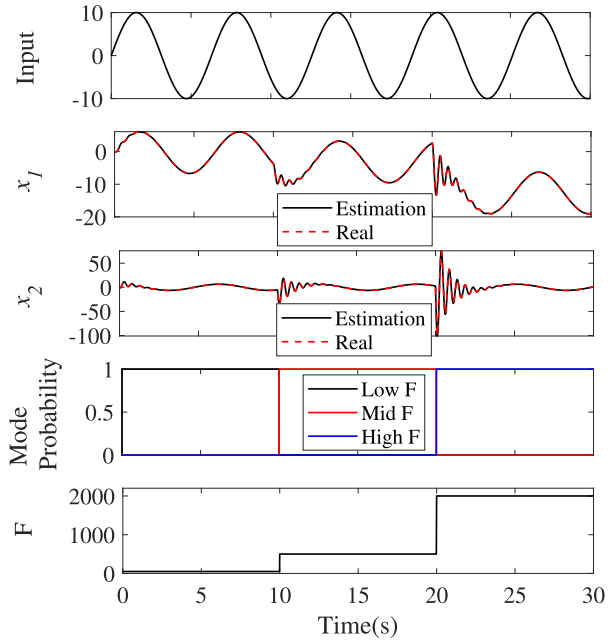

FIGURE 12. Identifying the external force for a second-order system with full-state feedback using IMM-KF.

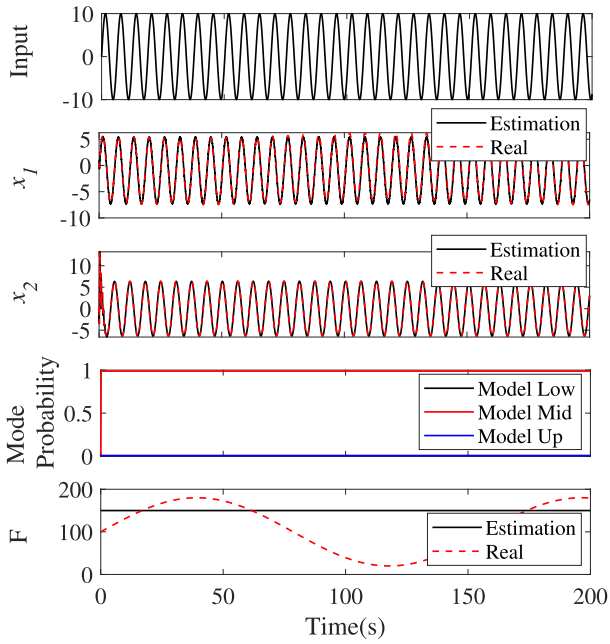

FIGURE 13. Identifying the time-varying external force for a second-order system with measurement feedback from x_2 using MWIMM-KF.

best performance when measurements for both states are available, which is intuitively reasonable.

Consequently, MWIMM is unable to accurately estimate the time-varying external force in cases where only the x_2 measurement is available, as depicted in Figs 13, 14 and 15. However, the external force estimation is achievable when either the x_1 measurement or both state measurements are available. Additionally, it is evident that the performance of MWIMM improves significantly when both states are measured, as the system exhibits a higher degree of observability.

A viable approach to address the identifiability concern in this scenario involves utilizing a robust filter, such as the Smooth Variable Structure Filter (SVSF), in lieu of the Kalman filter to account for model mismatch. An IMM-SVSF-VBL, equipped with a small boundary layer for the measured state and a large boundary layer for the unmeasured state, can effectively detect sudden changes in the external force by including additional information as follows:

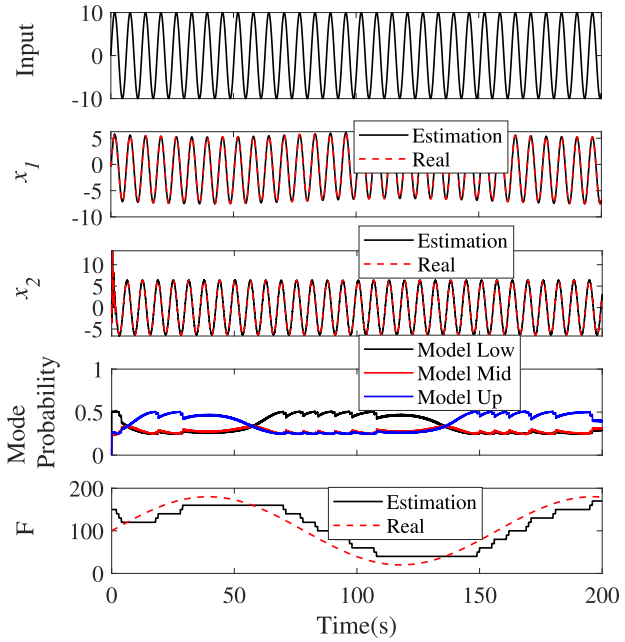

FIGURE 14. Identifying the time-varying external force for a second-order system with measurement feedback from x_1 using MWIMM-KF.

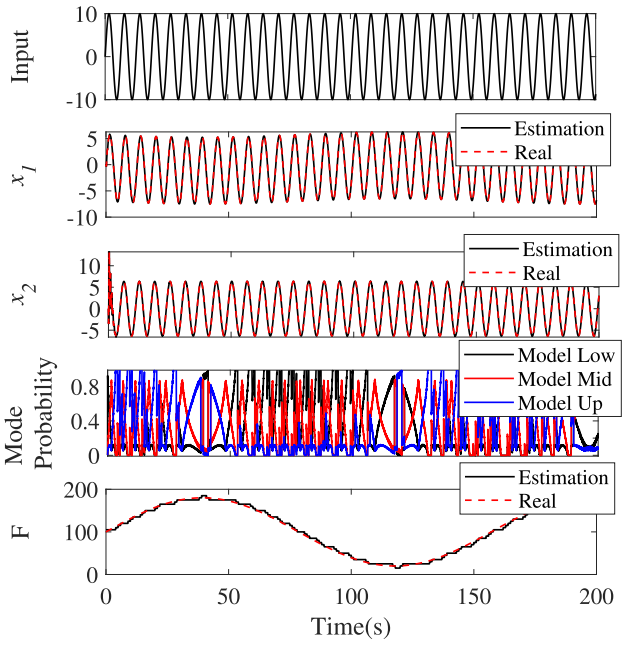

FIGURE 15. Identifying the time-varying external force for a second-order system with full-state using MWIMM-KF.

- By setting a small boundary layer threshold for the measured state x_2, the IMM-SVSF-VBL is capable of recognizing changes in the system model, triggering the corrective action of the SVSF.
- Conversely, a large boundary layer threshold for the unmeasured state x_1 implies that the system relies on the filter bank models to estimate the unmeasured state x_1, avoiding from correcting the a priori estimations of the filters based on new measurements. Consequently, the incorrect models maintain a substantial a priori error, helping the IMM to find the most relevant model.

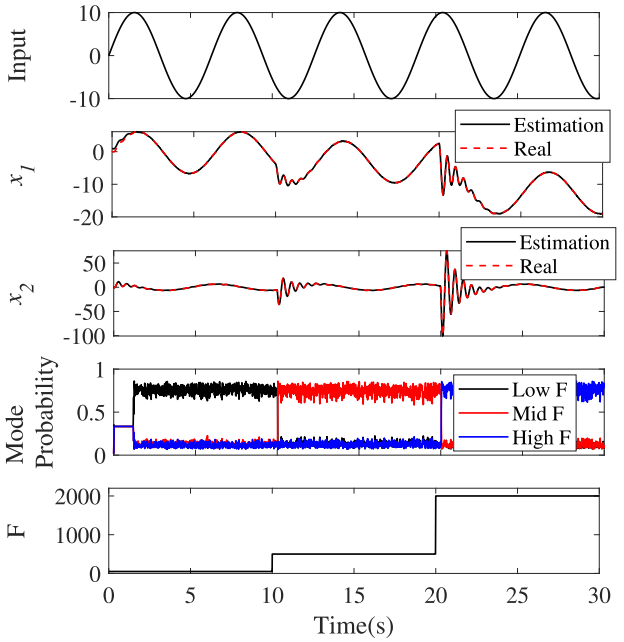

FIGURE 16. External load level identification in a second-order system form velocity measurement using IMM-SVSF-VBL; a sudden change in the external load level.

As depicted in Fig. 16, unlike IMM-KF, IMM-SVSF-VBL successfully identifies sudden changes in the level of the external force. However, as demonstrated in Fig. 17, it still struggles to identify the external force level when it changes gradually. In such cases, the slow deviation of the a priori error does not cross the boundary layer, giving the incorrect filter (representing a low external force model here) sufficient time to adjust the gain, to maintain a small a priori error, and prevent the IMM from switching. This limitation stems from the fact that the impact of a changing external force is akin to the displacement of a spring (x_1), and the filter cannot distinguish between the two solely based on the system's velocity measurement. This is due to the unobservability of the augmented state as shown in (26).

A. EXPLORING ROBUSTNESS

Another area worthy of further exploration is the robustness of the MWIMM algorithm. The Kalman filter utilized in the MWIMM algorithm, as discussed previously, assumes that the process and measurement noise of the system adhere to zero-mean and Gaussian distributions. Consequently, any bias or uncertainty present in the system can negatively impact the performance of this strategy, and in extreme cases, it may lead to instability of the Kalman filter. Considering the system in (13), let us assume the system behavior changes gradually over time due to variations in the damping ratio. Then, the MWIMM-KF strategy can be employed to estimate the damping ratio. To study the robustness of this approach, different levels of bias or uncertainty have been introduced to the natural frequency of the system. These scenarios are outlined below, and the results of the MWIMM-KF are presented in Fig. 18.

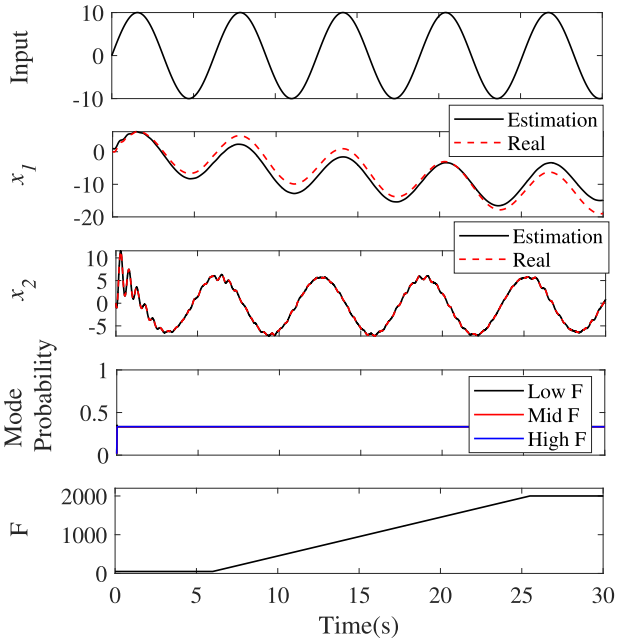

FIGURE 17. External load level identification in a second-order system form velocity measurement using IMM-SVSF-VBL; the gradual change in the external load level.

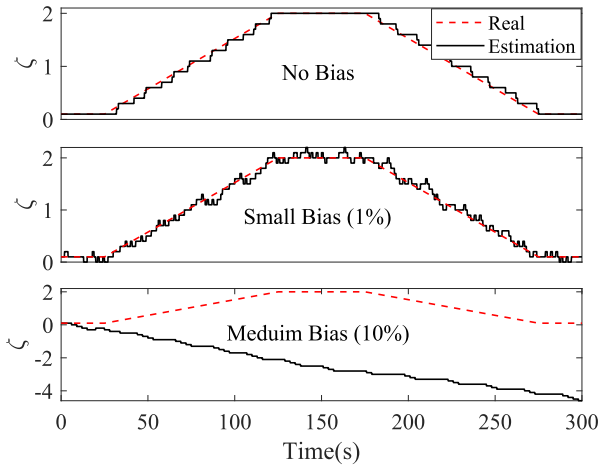

FIGURE 18. Using MWIMM-KF for estimating the time-varying parameter of a second-order system with different levels of bias or uncertainty.

1) System without bias or uncertainty: In this situation, the MWIMM-KF exhibits excellent performance as expected.
2) System with small bias or uncertainty (1% additive uncertainty): Despite a slight increase in estimation error compared to the scenario without bias, KF effectively manages to estimate states because the bias or uncertainty falls within the range of process noise.
3) System with medium bias or uncertainty (10% additive uncertainty): In this scenario, MWIMM-KF fails to estimate the damping ratio as the bias or uncertainty exceeds the range of process noise. Therefore, none of the models in the MWIMM window is capable of representing the system's behavior. MWIMM-KF tries to resolve this issue by switching to negative damping to adjust for the bias in natural frequency, which makes the problem even worse.
4) System with large bias or uncertainty (50% additive uncertainty): In this scenario, MWIMM-KF becomes unstable in less than 2 seconds as shown in Fig. 19.

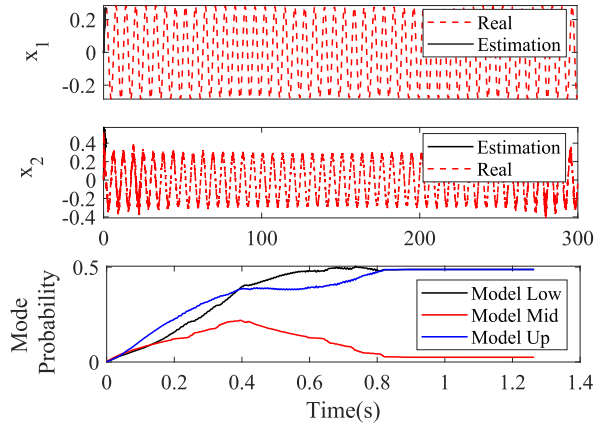

FIGURE 19. MWIMM-KF becomes unstable for estimating the time-varying parameter of a second-order system with large uncertainty (50% bias).

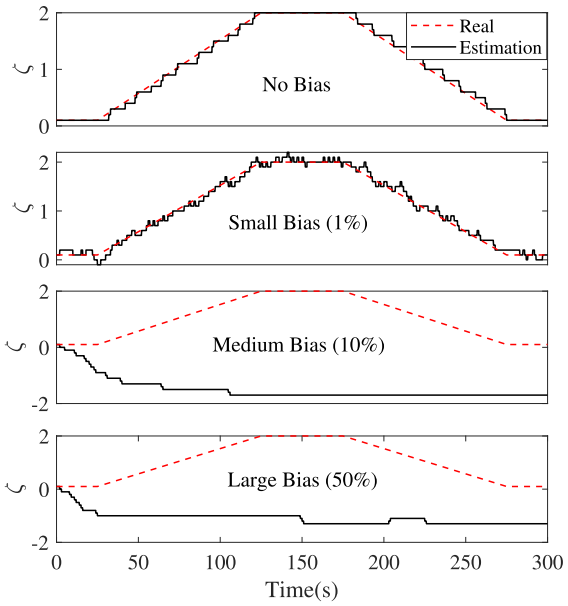

FIGURE 20. Using MWIMM-SVSF for estimating the time-varying parameter of a second-order system with different levels of bias or uncertainty.

One approach to improve robustness is to use a robust filtering strategy such as SVSF-VBL, instead of Kalman filter. Results for the same conditions using MWIMM-SVSF are illustrated in Fig. 20. These results are also compared with those of MWIMM-KF in Table. 2. In the scenario without bias, both KF and SVSF-VBL exhibit similar performance as expected. Note that employing a very small Fixed Boundary Layer (FBL) may compromise the performance of SVSF-VBL, as it relies on the fixed bound instead of the optimized one, which is calculated by taking account of system noise.

TABLE 2. Estimation errors with different bias/uncertainty levels.

Estimation Error No Bias	MWIMM-KF Normalized RMSE	MWIMM-SVSF Normalized RMSE
x_1	7.6419×10^{-4}	7.6419×10^{-4}
x_2	0.0056	0.0056
ζ	0.0311	0.0311
Estimation Error Small Bias/Uncertainty (1%)	MWIMM-KF Normalized RMSE	MWIMM-SVSF Normalized RMSE
x_1	7.6399×10^{-4}	7.6387×10^{-4}
x_2	0.0087	0.0345
ζ	0.0368	0.0376
Estimation Error Medium Bias/Uncertainty (10%)	MWIMM-KF Normalized RMSE	MWIMM-SVSF Normalized RMSE
x_1	5.8131×10^{-4}	7.6335×10^{-4}
x_2	0.2035	0.5365
ζ	37.3749	27.2272
Estimation Error Large Bias/Uncertainty (50%)	MWIMM-KF Normalized RMSE	MWIMM-SVSF Normalized RMSE
x_1	unstable	7.7567×10^{-4}
x_2	unstable	0.6884
ζ	unstable	22.8583

In the case of small bias, SVSF estimation error is slightly larger than KF, because corrective actions from FBL occur more frequently with a larger a priori error from uncertainty. Enhancing SVSF performance can be achieved by increasing FBL, but this comes at the expense of a larger error boundary.

For medium and large bias, MWIMM-SVSF fails to estimate the damping ratio. However, it ensures stability and boundedness of the estimation error. This is because when the prior error exceeds the fixed boundary layer, SVSF loses confidence in the model and relies on corrective actions from the fixed boundary layer. As a result, the estimation error of the damping ratio levels off.

As shown, although MWIMM-SVSF ensures the stability and boundedness of the estimation error, neither MWIMM-SVSF nor MWIMM-KF effectively captures the states and unknown parameters (e.g. damping ratio) under conditions of medium and large uncertainty. This outcome is expected, given that when uncertainty significantly outweighs the differences between model hypotheses, the comparison becomes irrelevant for identifying the true model. A more in-depth exploration of this issue could be pursued in the future, developing a robust estimation strategy based on the variable structure system concept, as demonstrated here. This could involve a comprehensive analysis of parameters such as bin size, window size, and process noise (Q) to enhance performance.

B. PRUNING STRATEGY

Instead of merging, an alternative for decreasing the number of regime sequences in MMAE algorithms involves employing pruning. Pruning entails the removal of low probability branches (i.e., regime sequences) from the MMAE tree, in contrast to the merging approach used in IMM. While merging algorithms such as IMM filters are widely employed in estimation tasks including target tracking, a pruning algorithm such as Multiple Model Pruning (MMP) [31] is more relevant for detecting changes in fault detection problems. In these scenarios, accurately identifying changes in the system's behavior is more important than estimating the system's state. The MMP algorithm has three main steps [31]:

1) Recursively compute the conditional filter for a bank of M sequences.
2) After the measurement update at time k, retain only the M/S most probable branches and prune the rest, S being the number of branches retained in each step.
3) At time $k+1$, allow the M/S considered branches to split into $S.M/S = M$ branches and update their a posteriori probabilities.

An entirely distinct approach to reduce the complexity and improve the performance of MMAE algorithms in addressing fault detection problems involves the adoption of the MMP algorithm. Future research may focus on exploring the pruning techniques as well as combining them and comparing them with merging approaches employed in this paper, such as IMM and MWIMM, for fault detection and diagnosis problems. One potential approach could involve implementing a moving window strategy to enhance the performance of an MMP algorithm.

VI. CONCLUSION

In this study, a novel adaptive estimation strategy called Mowing Window Interacting Multiple Model (MWIMM) has been introduced to address the challenges of state estimation in the presence of uncertain model parameters and changing system dynamics. Focusing on a subset of possible models at each stage instead of considering all models, MWIMM improves identifiability and computational efficiency by effectively narrowing down the search space for the true model. This approach enables the estimation of gradual changes in the system, making it particularly valuable for estimation of fault intensity and remaining useful life.

The parameter estimation problem was investigated, comparing the results obtained by the proposed method and the augmented state extended Kalman filter. The results demonstrated that the proposed MWIMM approach presents a promising alternative for effectively handling extensive parameter uncertainty and accommodating gradual changes in system parameters. Future research direction can focus on applying the proposed method to prognosis and degradation estimation problems, such as estimating the state of health of batteries.

REFERENCES

[1] Y. Bar-Shalom, X. R. Li, and T. Kirubarajan, *Estimation With Applications to Tracking and Navigation: Theory Algorithms and Software*. Hoboken, NJ, USA: Wiley, 2004.
[2] T. D. Barfoot, *State Estimation for Robotics*. Cambridge, U.K.: Cambridge Univ. Press, 2024.
[3] D. Ding, Q.-L. Han, X. Ge, and J. Wang, "Secure state estimation and control of cyber-physical systems: A survey," *IEEE Trans. Syst. Man, Cybern. Syst.*, vol. 51, no. 1, pp. 176–190, Jan. 2021.
[4] M. Athans and C.-B. Chang, *Adaptive Estimation and Parameter Identification Using Multiple Model Estimation Algorithm*. Lexington, MA, USA: MIT Lincoln Laboratory, 1976.
[5] M. Karasalo and X. Hu, "An optimization approach to adaptive Kalman filtering," *Automatica*, vol. 47, no. 8, pp. 1785–1793, Aug. 2011.
[6] S. Akhtar, P. Setoodeh, R. Ahmed, and S. Habibi, "A new strategy for combining nonlinear Kalman filters with smooth variable structure filters," *IEEE Access*, vol. 11, pp. 146262–146281, 2023.
[7] S. A. Gadsden, S. Habibi, and T. Kirubarajan, "Kalman and smooth variable structure filters for robust estimation," *IEEE Trans. Aerosp. Electron. Syst.*, vol. 50, no. 2, pp. 1038–1050, Apr. 2014.
[8] S. Habibi, "The smooth variable structure filter," *Proc. IEEE*, vol. 95, no. 5, pp. 1026–1059, May 2007.
[9] A. Saeedzadeh, P. Setoodeh, M. Alavi, and S. Habibi, "Information extraction using spectral analysis of the chattering of the smooth variable structure filter," *IEEE Access*, vol. 11, pp. 104992–105008, 2023.
[10] M. Al-Shabi, S. A. Gadsden, and S. R. Habibi, "Kalman filtering strategies utilizing the chattering effects of the smooth variable structure filter," *Signal Process.*, vol. 93, no. 2, pp. 420–431, Feb. 2013.
[11] D. Simon, *Optimal State Estimation: Kalman, H Infinity, and Nonlinear Approaches*. Hoboken, NJ, USA: Wiley, 2006.
[12] M. S. Grewal and A. P. Andrews, *Kalman Filtering: Theory and Practice With MATLAB*. Hoboken, NJ, USA: Wiley, 2014.
[13] L. Ljung, "Asymptotic behavior of the extended Kalman filter as a parameter estimator for linear systems," *IEEE Trans. Autom. Control*, vols. AC-24, no. 1, pp. 36–50, Feb. 1979.
[14] L. Nelson and E. Stear, "The simultaneous on-line estimation of parameters and states in linear systems," *IEEE Trans. Autom. Control*, vols. AC-21, no. 1, pp. 94–98, Feb. 1976.
[15] P. Abbeel, A. Coates, M. Montemerlo, A. Y. Ng, and S. Thrun, "Discriminative training of Kalman filters," *Robot., Sci. Syst.*, vol. 2, pp. 1–13, Sep. 2005.
[16] A. Saeedzadeh, S. Habibi, M. Alavi, and P. Setoodeh, "A robust model-based strategy for real-time fault detection and diagnosis in an electro-hydraulic actuator using updated interactive multiple model smooth variable structure filter," *J. Dyn. Syst., Meas., Control*, vol. 145, no. 10, pp. 1–23, Oct. 2023.
[17] A. Saeedzadeh, S. Habibi, and M. Alavi, "A model-based FDD approach for an EHA using updated interactive multiple model SVSF," in *Fluid Power Systems Technology*, vol. 85239. New York, NY, USA: American Society of Mechanical Engineers, 2021.
[18] A. Saeedzadeh, "Dynamic model-based estimation strategies for fault diagnosis," Ph.D. dissertation, Mech. Eng. Dept., McMaster Univ., Hamilton, ON, Canada, 2024.
[19] Y. Lu, H. Ma, E. Smart, and H. Yu, "Real-time performance-focused localization techniques for autonomous vehicle: A review," *IEEE Trans. Intell. Transp. Syst.*, vol. 23, no. 7, pp. 6082–6100, Jul. 2022.
[20] F. Tufano, D. G. Lui, S. Battistini, R. Brancati, B. Lenzo, and S. Santini, "Vehicle sideslip angle estimation under critical road conditions via nonlinear Kalman filter-based state-dependent interacting multiple model approach," *Control Eng. Pract.*, vol. 146, May 2024, Art. no. 105901.
[21] T. Kirubarajan, Y. Bar-Shalom, K. R. Pattipati, and I. Kadar, "Ground target tracking with variable structure IMM estimator," *IEEE Trans. Aerosp. Electron. Syst.*, vol. 36, no. 1, pp. 26–46, Jan. 2000.
[22] C. Kim, F. Li, A. Ciptadi, and J. M. Rehg, "Multiple hypothesis tracking revisited," in *Proc. IEEE Int. Conf. Comput. Vis. (ICCV)*, Dec. 2015, pp. 4696–4704.
[23] M. Efe and D. P. Atherton, "The IMM approach to the fault detection problem," *IFAC Proc. Volumes*, vol. 30, no. 11, pp. 603–608, Jul. 1997.
[24] S. A. Gadsden, Y. Song, and S. R. Habibi, "Novel model-based estimators for the purposes of fault detection and diagnosis," *IEEE/ASME Trans. Mechatronics*, vol. 18, no. 4, pp. 1237–1249, Aug. 2013.
[25] A. S. Lee, Y. Wu, S. A. Gadsden, and M. AlShabi, "Interacting multiple model estimators for fault detection in a magnetorheological damper," *Sensors*, vol. 24, no. 1, p. 251, Dec. 2023.
[26] Y. Zhang and J. Jiang, "Integrated active fault-tolerant control using IMM approach," *IEEE Trans. Aerosp. Electron. Syst.*, vol. 37, no. 4, pp. 1221–1235, Aug. 2001.
[27] M. Kheirandish, E. A. Yazdi, H. Mohammadi, and M. Mohammadi, "A fault-tolerant sensor fusion in mobile robots using multiple model Kalman filters," *Robot. Auto. Syst.*, vol. 161, Mar. 2023, Art. no. 104343.
[28] C. Sun, Y. Lin, and L. Li, "Intermittent monitoring-based adaptive fault-tolerant control for uncertain nonlinear systems with actuator switching," *Int. J. Robust Nonlinear Control*, vol. 34, no. 8, pp. 5063–5078, May 2024.
[29] Y. Baram and N. Sandell, "Consistent estimation on finite parameter sets with application to linear systems identification," *IEEE Trans. Autom. Control*, vols. AC-23, no. 3, pp. 451–454, Jun. 1978.
[30] H. Bozdogan, "Model selection and Akaike's information criterion (AIC): The general theory and its analytical extensions," *Psychometrika*, vol. 52, no. 3, pp. 345–370, Sep. 1987.
[31] F. Gustafsson and F. Gustafsson, *Adaptive Filtering and Change Detection*, vol. 1. Hoboken, NJ, USA: Wiley, 2000.

AHSAN SAEEDZADEH received the B.S. and M.S. degrees in mechanical engineering from the Amirkabir University of Technology, Tehran, Iran, in 2013 and 2016, respectively. He is currently pursuing the Ph.D. degree in mechanical engineering with McMaster University, Hamilton, ON, Canada.

From 2012 to 2016, he was a Research Assistant with the Robotics and Automation Laboratory, New Technology Research Center (NTRC), Tehran. He devoted three years to his role as a Mechanical Engineer within an Iranian start-up enterprise. His research interests include fault detection and diagnosis, state estimation, dynamic control, signal processing, and fluid power control. He was a recipient of the Merit-Based Admission to the Master of Science Program by the Honors Center, Tehran Polytechnic.

PEYMAN SETOODEH (Senior Member, IEEE) received the B.Sc. and M.Sc. degrees (Hons.) in electrical engineering from Shiraz University and the Ph.D. degree in computational engineering and science from McMaster University. He was the Harrison McCain Visiting Professor with the Marine Additive Manufacturing Centre of Excellence (MAMCE), University of New Brunswick, and an Associate Professor with the School of Electrical and Computer Engineering, Shiraz University. He was a Senior Research Engineer with the Huawei Noah's Ark Laboratory and a Lecturer with the Department of Electrical and Computer Engineering, McMaster University. He is currently with the Centre for Mechatronics and Hybrid Technologies (CMHT), McMaster University. He has co-authored two books, such as *Fundamentals of Cognitive Radio* and *Nonlinear Filters: Theory and Applications*. He is the co-author of an article on "Cognitive Control," which was featured as the cover story of PROCEEDINGS OF THE IEEE in the December issue of the centennial year. His research interests include cognitive systems, artificial intelligence, quantum control, and nonlinear estimation. He was a recipient of the Monbukagakusho Scholarship from the Ministry of Education, Culture, Sports, Science, and Technology, Japan.

MARJAN ALAVI (Senior Member, IEEE) received the B.Sc. degree in electrical engineering (control and instrumentations) from the K. N. Toosi University of Technology, the M.Sc. degree in Electrical Engineering (micro- and nano-electronic devices) from the Sharif University of Technology, and the Ph.D. degree in electrical engineering from Nanyang Technological University (NTU), Singapore.

In 2015, she joined the Energy Systems Group, Department of Electrical and Computer Engineering, University of Toronto, as a Postdoctoral Fellow. She is currently the Chair of the Manufacturing Engineering Master of Engineering (MEME) Program, W. Booth School of Engineering Practice and Technology (SEPT), McMaster University, Canada. She is also an Assistant Professor with SEPT teaching in two Bachelor of Technology (B.Tech.) programs: Automation Engineering Technology Program and Software Technology - Degree Completion Program (DCP). She is also an Associate Member of the Mechanical Engineering and Computer and Electrical Engineering Departments, McMaster University. She has several years of industrial experience as an Electrical Engineer. She has been teaching several courses in electrical engineering at college and university levels, including digital electronics, embedded systems, the Internet of Things (IoT), artificial intelligence (AI), and smart cities. Her research interests include model-based and data-driven approaches for the diagnosis and prognosis of hybrid systems.

Dr. Alavi was a recipient of Singapore International Graduate Award (SINGA), in 2010. She has served on the IEEE Toronto Executive Committee as the Treasurer for four years, from 2016 to 2020. She has served as the Vice Chair for the IEEE Industrial Applications Society, in 2015, and the Vice Chair of Women in Engineering (WIE), from 2018 to 2022. She is the Chair of the Women in Engineering Affinity Group in Hamilton Section, Canada. She was a Reviewer of IEEE TRANSACTIONS ON INDUSTRIAL ELECTRONICS. She is the Guest Editor of *Frontiers on the Internet of Things*. She is a Professional Engineer in the province of Ontario, Canada.

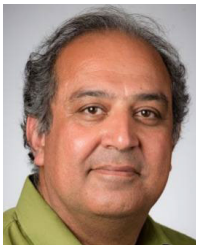

SAEID HABIBI (Member, IEEE) received the Ph.D. degree in control engineering from the University of Cambridge, U.K., in 1990. He has considerable managerial and industrial experience. He spent several years in the industry as a Project Manager and a Senior Consultant with Cambridge Control Ltd., U.K., where he was involved in automotive and aerospace-related projects. In Canada, he was with AlliedSignal Aerospace (presently part of Honeywell) where his last appointment was as a Senior Department Manager of systems engineering. He has received corporate training in both functional and program management. In 2006, he joined McMaster University, where he was the Chair of the Department of Mechanical Engineering, from 2008 to 2013. He is a Tier I Canada Research Chair and previously a Senior NSERC Industrial Research Chair (IRC) (from 2011 to 2022, renewed in 2016). He is currently the Founder and the Director of the Centre for Mechatronics and Hybrid Technologies. He is a full-time Professor with the Department of Mechanical Engineering, McMaster University. He is the Founder and the CEO of EECOMOBILITY Inc., which is a Canadian start-up out of McMaster University, specializing in battery testing and characterization, and AI software, and has developed unique test and monitoring products. EECOMOBILITY's products are applicable to batteries, the automotive sector, and electrified powertrains. His extensive technical background includes research into battery modeling and control, state and parameter estimation, mechatronics engineering, fault diagnosis and prognosis, advanced electric drive vehicles, vehicular power and propulsion systems, and energy and sustainability. He has a strong track record of HQP supervision, including 22 Ph.D. and 46 master's students, 13 PDFs, and 14 Research Engineers; many of whom have risen to senior positions in industry, and four have faculty positions. He has over 200 publications in some of the top journals and three patents. He is a fellow of the American Society of Mechanical Engineers (ASME) and a fellow of the Canadian Society of Mechanical Engineers (CSME). He was a recipient of several awards. He and his colleagues received the 2012 Best Paper Prize from the IEEE Transportation Electrification Conference for the application of their SVSF theory to condition monitoring of battery cells. He received two corporate awards for his contributions to the AlliedSignal Systems Engineering Process. He was a recipient of the Institution of Electrical Engineers (IEE) F. C. Williams Best Paper Award for his contribution to the variable structure systems theory.